Hyperfine Interact
DOI 10.1007/s10751-013-0831-8

# Structural and magnetic characterization of the "GASPAR" meteorite from Betéitiva, Boyacá, Colombia

**L. M. Flor Torres · G. A. Pérez Alcazar**



**Abstract** A structural and magnetic characterization has been performed of a plate obtained from the "Gaspar" meteorite from the Otengá region of the Betéitiva municipality, Boyacá, Colombia. The sample was provided by Ingeominas (Colombian Geological Agency). After the studies the sample was classified as an octahedral iron meteorite, due the Fe and Ni concentrations and the Widmanstätten pattern which was observed on the surface of the sample. The plate shows a crack which divides the sample in two regions (side A and B, respectively). Both sides were studied using techniques like X-rays diffraction (XRD), Mössbauer spectrometry, optical microscopy, and scanning electronic microscopy (with EDAX). On both sides an iron Fe-Ni matrix (kamacite) was found; a large quantity of carbon in the form of graphite and in two types: nodular and laminar; and different preferential orientation in both sides of the sample. The studies permit to prove that Gaspar is a fragment of the registered Santa Rosa de Viterbo meteorite.

**Keywords** Fe-Ni iron meteorite · X-ray diffraction · Mössbauer spectrometry · Optical microscopy · Scanning electron microscopy

## 1 Introduction

There are extraterrestrial bodies of different sizes traveling in space named meteors. These are produced due the degradation of the surface of bodies like asteroids, comets or inclusive planets different to the earth.

Proceedings of the thirteenth Latin American Conference on the Applications of the Mössbauer Effect, (LACAME 2012), Medellín, Columbia, 11–16 November 2012.

L. M. Flor Torres (✉) · G. A. Pérez Alcazar
Departamento de Física, Universidad del Valle, A.A. 25360, Cali, Colombia
e-mail: lauren.flor.univalle@gmail.com

Published online: 13 March 2013

**Table 1** Textural classification of metallic meteorites based in the Ni percentage [2]

| Class | Symbol | Strip thickness (mm) | %Ni |
|---|---|---|---|
| Hexahedrite | H | >50 | 4.5–6.5 |
| Octhahedrite | O | | |
| Very thick | Ogg | 3.3–50 | 6.5–7.2 |
| Thick | Og | 1.3–3.3 | 6.5–7.2 |
| Medium | Om | 0.5–1.3 | 7.4–10.3 |
| Fine | Of | 0.2–0.5 | 7.8–12.7 |
| Very fine | Off | <0.2 | 7.8–12.7 |
| Plassitic | Opl | <0.2 | 12.7–16.0 |
| Ataxite | D | Ausente | >16.0 |

When these bodies enter in contact with the earth atmosphere, before they strike the earth surface, they lose mass due the strong friction with the atmosphere, and in this way they lose kinetic energy which is transformed in light and heat, forming in this way the as called fugal start or meteor. Those meteors which have a mass above some tens of kilograms can survive the travel across the atmosphere and impact the earth surface and are called meteorites [1].

Meteorites can be classified in three groups, depending on their composition [1]: stony, iron, and stony-iron meteorites. The stony ones principally consist of olivine, pyroxene, feldspar, and in some cases they can present iron and nickel in small proportions. This group is divided in two subgroups: the stony meteorites which contain chondrules, called chondrites and those without chondrules called achondrites.

The second group is also named metallic or siderites. They consist for more than 90 % of Fe-Ni alloys like Kamacite (4–7 at. % of Ni) and Taenite (20–45 at. % of Ni), which present the so called Widmanstätten pattern. This type of meteorites can also contain other minerals like troilite, graphite, coenite and some silicates, in non-considerable amounts.

The textural classification of the iron meteorites is based in the width of the Kamacite plates in the Widmanstätten texture [2]. This width depends on the Ni content of the meteorite (Table 1).

The third group or stony-iron meteorites are also known as sideralites. They are bodies composed by iron-nickel phases and silicates, in approximately similar fractions.

The meteorite object of present study (see Fig. 1), was found in the Otengá region, Betéitiva municipality, Boyacá Department, Colombia, by peasants of the region during their land preparation labors for corn sowing. They collected this sample because it was a different material than those normally found in the zone, and it was transported to INGEOMINAS (Colombian Geologic Agency) of Boyacá. This meteorite was named "Gaspar".

The aim of this paper is to report the analysis performed on the "Gaspar" meteorite, by using X-ray diffraction, Mössbauer spectrometry, optical microscopy, and scanning electron microscopy (including EDAX). These results will be compared with previous ones reported for other meteorites found in neighboring zones in order to know if this is a part of the same sample or is a body of different origin.

Previous studies conducted in some bodies found in neighboring zones of the site in which the Gaspar meteorite was found, like Santa Rosa de Viterbo, Rasgatá, and others [2–4], reported that the samples are part of the registered Santa Rosa de

**Fig. 1** "Gaspar" meteorite found in Betéitiva. Boyacá

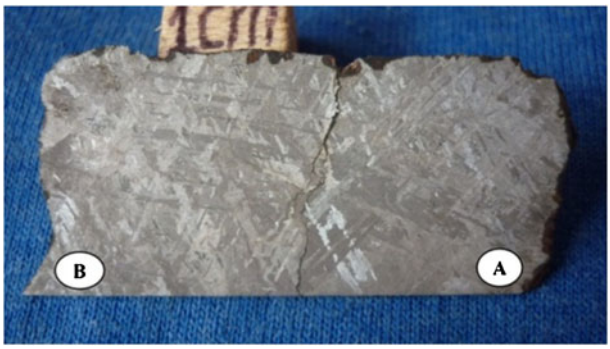


**Fig. 2** Widmanstätten pattern of the plate cutted from the GASPAR meteorite. A crack divides the sample in two regions

Viterbo meteorite [5], which presents an elemental composition near 91 at. % Fe, 7 at. % Ni and nearly 2 at. % of silicates.

## 2 Experimental

Initially a plate of nearly 0,6 cm width was cut, using the *IsoMet® 5000 Family of Linear Precision Saws* cutter,of the Universidad del Valle. This plate was polished with sandpapers of different grades (220, 320, 360, 400, 600, 1200, and 2000), until a specular surface was obtained. Then it was attacked with nital and the Widmanstätten pattern was obtained. Also the crack which divides the plate in two zones was present. These two zones were studied and analyzed (see Fig. 2).

### 2.1 Optical microscopy results

The optical microscopy analysis was realized by using the equipment of the Materials School of Universidad del Valle, and permitted to observe the different grain sizes on both sides of the sample, and also the different orientations of the Widmanstätten pattern (Fig. 3).

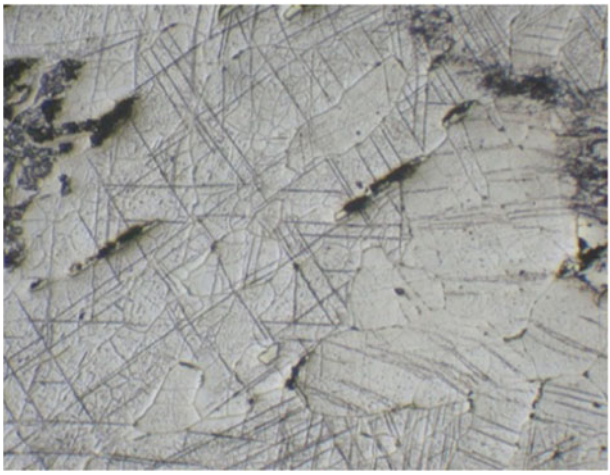

**Fig. 3** Optical microscopy picture of the A side of the GASPAR meteorite showing the different orientations of the Widmanstätten pattern

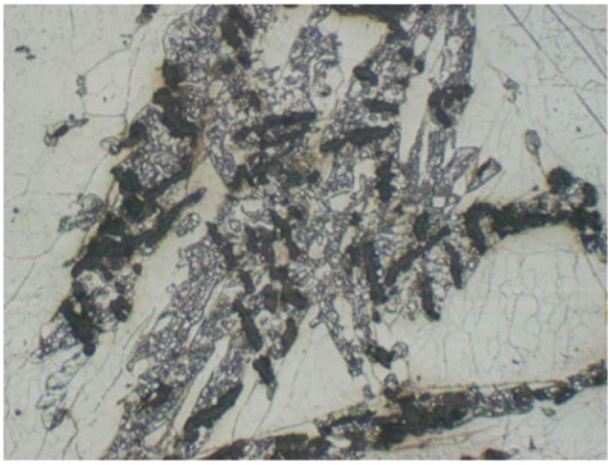

**Fig. 4** Optical microscopy picture of bright, dark, and clear zones of side B

Different microstructures (see Fig. 4) were found of bright, dark, and clear zones. These microstructures were found in different zones of both sides of the sample.

## 2.2 Scanning Electron Microscopy results (SEM and EDAX)

The JEOL JSM-6490LV scanning electron microscopy of the materials school of Universidad del Valle, with an INCA PENTAFE×3 OXFORD prove, was used.

With this equipment the Widmanstätten pattern was observed with bigger resolution and some particles were observed inside the lines of the pattern (Fig. 5). Besides these particles, some dark zones were additionally found, as shown in Fig. 6.

The analysis by EDAX shows that both regions of the dark zone (1 and 2 of Fig. 6), present a similar composition. Fe is present with ~45 wt. %, C presents a weight of

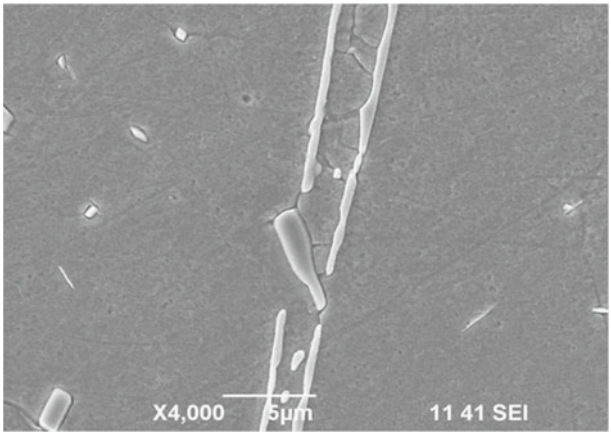


**Fig. 5** SEM micrograpy of side A of the sample. It shows a magnification of the Widmanstätten pattern, with some particles inside

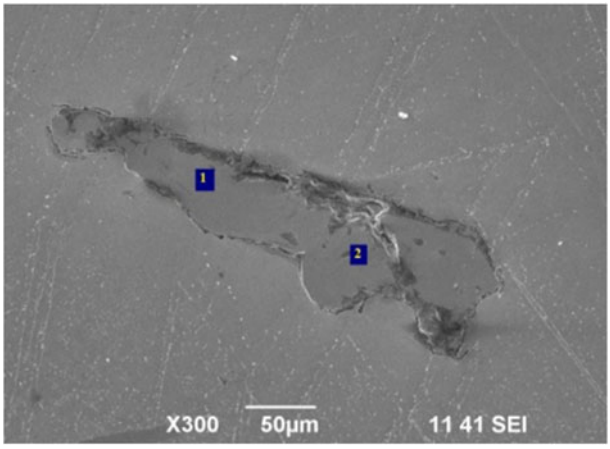


**Fig. 6** Dark zone found in the B side of the sample

∼23 %, Ni presents a weight of ∼20 %, and P is present with a weight of ∼10 %. These dark regions were found in both sides of the sample.

Using EDAX it was possible to find the chemical composition of the bright and dark zones detected by optical microscopy of Fig. 4.

The dark zones present a mean composition, which is similar in both sides, with ∼94 wt. % of C and ∼5 wt. % of O. This composition indicates that these zones may correspond to graphite. The bright zones present a composition similar in both sides of the sample with ∼55 wt. % Fe, ∼25 wt. % of C, and small quantities of Ni, P, and O. The morphology and composition of these zones permit to attribute them to perlite. However, as can be seen in Fig. 7a and b, the shape of the graphite is not the same at both sides of the sample. It is present as laminar (side B) and nodular (side A) types. According with the metallurgical process followed for heat treatment of iron-carbon steels, the lamellar graphite can be formed if the furnace temperature is maintained between 900 and 955 °C, followed by cooling down to 300 °C during two hours (higher cooling rate). The conditions for the formation

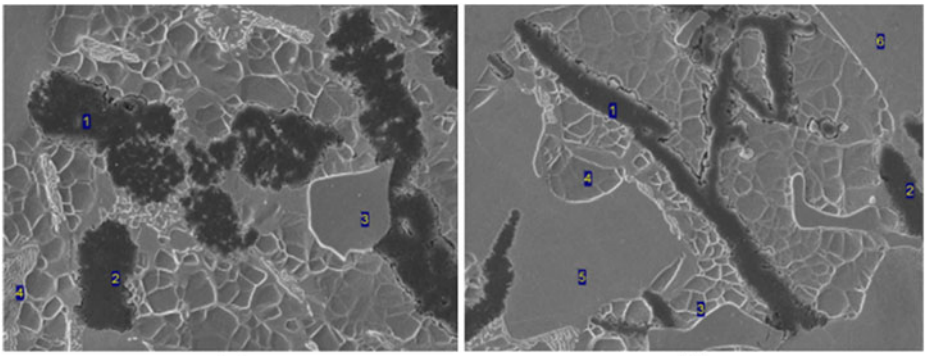


**Fig. 7** SEM pictures of **a** bright and dark zones of side A (×1000), and **b** bright and dark zones of side B of the sample (×1000)

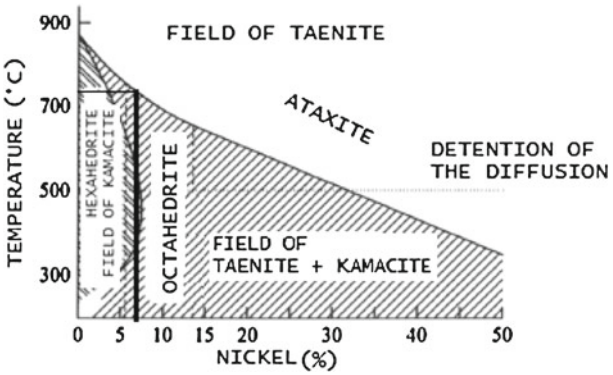


**Fig. 8** Phase stability diagram of the different Fe-Ni phases [2]

of nodular graphite are: temperature of the furnace maintained between 915 and 930 °C, and followed by cooling down to 700 °C during two hours (smaller cooling rate). Taking into account that meteorites maintain a very low temperature until they reach the upper layers of the atmosphere, when they come into contact with these upper layers, an increase in temperature is produced due to the friction between the meteorite and the atmosphere, volatizing partially or completely if the meteorite is very small. The higher temperature corresponds to that side which is in friction with the atmosphere, producing a different heating and cooling regime to that of the other side of the meteorite, explaining in this way the formation of the nodular graphite in side A and the laminar one in side B. When the meteorite falls on the earth it cools further, reaching its coldest temperature at the earth.

Compositional analysis was also performed to the matrix of both sides of the meteorite. The same three elements were found in both sides, Fe with near 70.65 wt. %, C with near 24.69 wt. %, and Ni with near 4.67 wt. % in the side A and 70.07 wt. % of Fe, 24.54 wt. % of C and 5.39 wt % of Ni in the side B. According to this composition the meteorite can be classified as iron or metallic, and the composition is nearly the same at both sides.

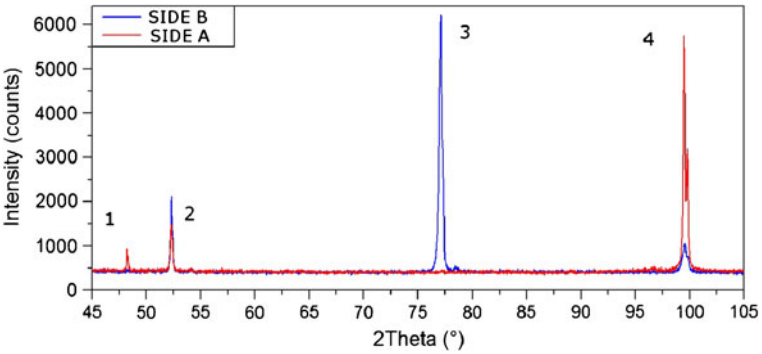


**Fig. 9** XRD patterns of both sides of the GASPAR meteorite. *Red line* corresponds to the Side A and *blue line* to the side B

**Table 2** Results of the crystallographic analysis of side A of the "GASPAR" meteorite

| Parameters | Phase 1 - C | Phase 2 - $\alpha$Fe10.8Ni |
|---|---|---|
| Crystallite size $\perp$ [nm] | 280.11 | 93.12 |
| Crystallite size $\parallel$ [nm] | 280.11 | 93.12 |
| a – b – c [Å] | 2.470 – 2.470 – 6.800 | 2.872 |
| $\alpha - \beta - \gamma$ [°] | 90 – 90 – 120 | 90 |
| Lattice | Hexagonal | Cubic |
| Symmetry | 6/mmm(6/m2/m2/m) | m3m (4/m32/m) |

**Table 3** Results of the crystallographic analysis of side B of the "GASPAR" meteorite

| Parameters | Phase 1 - C | Phase 2 - $\alpha$Fe10.8Ni |
|---|---|---|
| Crystallite size $\perp$ [nm] | 1142.45 | 67.30 |
| Crystallite size $\parallel$ [nm] | 5.80 | 199.63 |
| a – b – c [Å] | 2.524 – 2.524 – 4.471 | 2.871 |
| $\alpha - \beta - \gamma$ [°] | 90 – 90 – 120 | 90 |
| Lattice | Hexagonal | Cubic |
| Symmetry | 6/mmm(6/m2/m2/m) | m3m (4/m32/m) |

The approximate weight concentration values, in the matrix, for nickel and iron are 5.04 and 70.36 %, respectively. The total nickel concentration, for comparison and classification of the samples in the different subgroups of metallic meteorites, is obtained by the equation

$$Ni_T = \frac{Ni}{Fe + Ni}\% \tag{1}$$

The obtained total weight value for nickel was ~6.68 %. Comparing this value to those required in each subgroup of meteorites, the "GASPAR" meteorite is classified as an octahedrite (Og) IIIAB type.

In the stability phase diagram of the different Fe-Ni phases (Fig. 8), it can be observed that a material with Ni between ~7 and 14 wt. %, can be classified in the

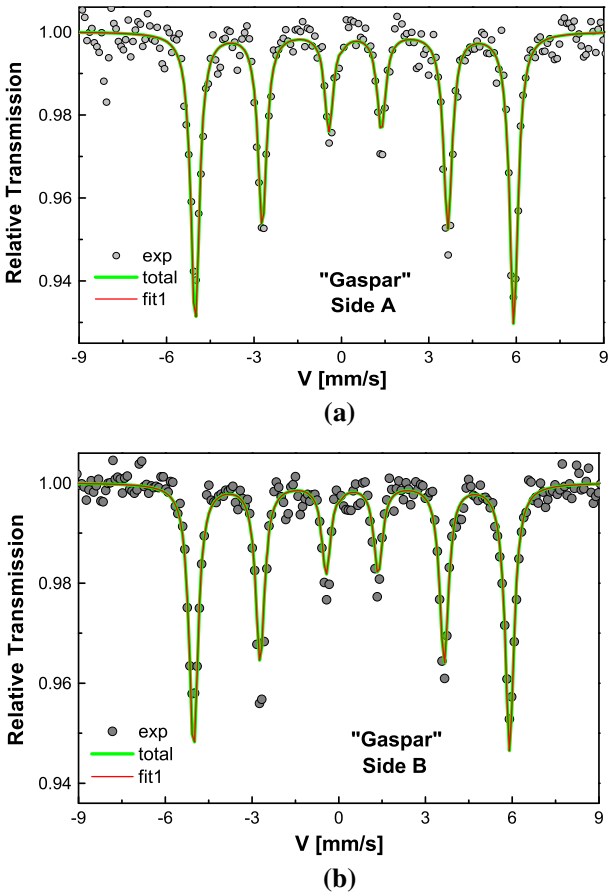


**Fig. 10** Mössbauer spectra of both sides of the "GASPAR" meteorite, **a** side A of the sample, and **b** side B of the sample

octahedrite meteorite group with Kamacite presence. According to its composition GASPAR meteorite is part of this group [6]. Besides, the associated temperature is less than 900 °C.

## 2.3 X-ray diffraction (XRD) results

The XRD patterns of both sides of the sample were refined by using the Rietveld method with the GSAS program [7], and the line sequence of the $\alpha$-$Fe_{10.8}Ni$ (BCC) and carbon phases like Lonsdaleite (side A) and Graphite (side B). The patterns are shown in Fig. 9 and the refined parameters are shown in Tables 2 and 3.

Two differences in the peak intensities can be observed. The first one is in the intensities of the peaks 2 and 4 of the pattern, which correspond to the (110) and (211) of the $\alpha$-$Fe_{10.8}Ni$ phase. In phase B the contribution of peak 2 is larger and for peak 4 the larger contribution is found on side A. The second one is that the intensity of the peak 1, which corresponds to the carbon phases, is dominating on side B. These results show that the different thermal regimens of both sides induce

**Table 4** Mössbauer parameters obtained for both sides of the GASPAR meteorite

| | DI (mm/s) | SQ (mm/s) | H (kOe) |
|---|---|---|---|
| Side A | 0.009 ± 0.667E-02 | −0.022 ± 0.916E-02 | 337.1 ± 0.3 |
| Side B | 0.004 ± 0.567E-02 | −0.022 ± 0.719E-02 | 337.1 ± 0.3 |

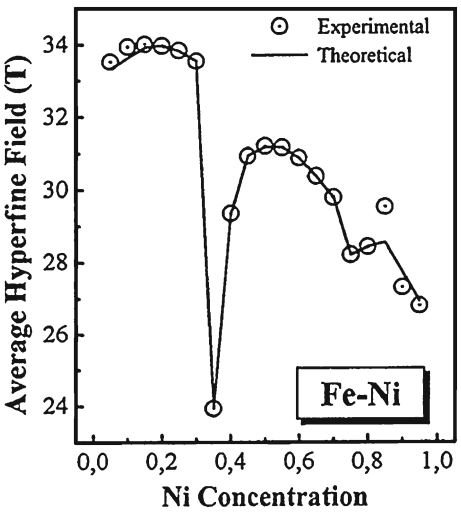


**Fig. 11** Dependence of the mean hyperfine field with the Ni concentration (figure taken from Ref. [8])

different preferential orientations in them. After the refinement of the two patterns the following crystallographic parameters were obtained:

It can be noted that graphite (Phase 1-C) of side A presents crystallite sizes parallel and perpendicular with similar values (≈280 nm), in according with the nodular morphology detected by SEM. Besides, the obtained graphite in size B presents a perpendicular crystallite size (≈1142 nm) much bigger than that of the parallel size (≈6 nm) showing its lamellar shape in according with the SEM results.

## 2.4 Mössbauer spectrometry studies

The Mössbauer spectra of both sides of the sample are shown in Fig. 10. In Table 4 the hyperfine parameters are listed obtained after the fitting of the spectra. It can be observed that the isomer shift and the quadrupole splitting of the obtained sextet correspond to those of iron, however the hyperfine field obtained is near 337 kOe, then it is bigger than that of pure iron.

This larger hyperfine field can be attributed to the substitution of Fe atoms by Ni atoms, because this substitution increase the mean hyperfine field as was reported by Restrepo et al. [8]. They proved that the mean hyperfine field of Fe-Ni alloys increases when the Ni content increases between 0 up to 20 at. % (see Fig. 11). Our material presents a Ni concentration around 5 wt. %, and is the region of larger mean hyperfine fields (Fe and Ni present nearly the same weight).

## 3 Conclusions

The GASPAR meteorite was classified as an iron meteorite or metallic octahedrite (Og) IIIAB type, due to the presence of a Widmanstätten pattern typical of these meteorites, a concentration of nickel of 6.6 wt. %, and the Kamacite and Taenite phases. Besides, its matrix contains a majority content of Fe, C, and Ni in both sides of the sample.

With the help of the stability phase diagram of the Fe-Ni alloys, it was possible to observe that a material with 6.6 wt. % is inside the field of the octahedrite with a temperature below 900 °C, and these conditions are those of the GASPAR meteorite.

The different types of graphite found in both sides of the meteorite and the different texture of then, permit to conclude that both sides were exposed to different heating and cooling regimes when one side was exposed more directly to the friction with the earth's atmosphere before the impact.

The increase in the hyperfine field (370 kOe) compared to that of pure iron is due to the percentage of Ni that is in the BCC material.

Comparing our results with previous studies, it can be said that this meteorite has very similar characteristics to those found and studied in other fragments collected in nearby areas, so it is possible that Gaspar meteorite is part of the Santa Rosa of Viterbo meteorite, found in Boyáca, Colombia, near the site in which Gaspar was found.

**Acknowledgements** The authors would like to thank Mr. Jaime H. Toro, owner of GASPAR meteorite, from La Pradera community, and Dr. Jose Arenas, Director of the Ingeominas Geological Museum in Bogotá who permitted the GASPAR study. We also thank Universidad del Valle and the CENM-Univalle by the financial support.

## References

1. Lamus, C.M., Medina, B.: Meteoritos: petrografía, geoquímica y origen astrofísico. Medellín, Thesis, Colombia (2002)
2. Gil, J., Concha, A.: Caracterización petrográfica y clasificación textural del meteorito de Santa Rosa de Viterbo (Boyacá), Colombia. Geol. Colomb. No. 31, ISSN 0072-0992, (2006)
3. Ramirez, J.E.: Meteors and meteorites. Contributions of the Meteoritical Society. The Meteorites of Santa Rosa de Viterbo, Boyacá, Colombia (730,059), vol. LVII, pp. 29–36. Instituto Geofísico de los Andes Colombianos, Bogotá, Colombia (1949)
4. Buchwald, V.F., Wasson, J.T.: The two colombian iron meteorites, Santa Rosa and Tocavita. Analecta Geol. **3**, 5–29 (1968)
5. Meteoritical Society: "Santa Rosa". Year found: 1810. Page on the Internet: http://www.lpi.usra.edu/meteor/metbull.php?code=23167
6. Norton, O.R.: The Cambridge Encyclopedia of Meteorites, pp. 354. Cambridge University Press, UK (2002)
7. Larson, C.A., Von Dreele, R.B.: GSAS, General Structure Analysis System. Los Alamos National Laboratory, Los Alamos (2004)
8. Restrepo, J., Pérez Alcázar y, G.A., Bohórquez, A.: Description in a local model of the magnetic field distributions of $Fe_{1-x}Ni_x$ disordered alloys. J. Appl. Phys. **81**, 4101 (1997)